Cell Reports, Volume *32*

Supplemental Information

Control of Viral Infection by Natural Killer Cell Inhibitory Receptors

Bijal A. Parikh, Michael D. Bern, Sytse J. Piersma, Liping Yang, Diana L. Beckman, Jennifer Poursine-Laurent, Béatrice Plougastel-Douglas, and Wayne M. Yokoyama

Supplementary Figure Legends

Figure S1. Characterization of on-target and off-target CRISPR deletions targeting specific *Ly49* genes. Genomic DNA was isolated from back-crossed H2D^{d} CRISPR-Cas9 modified mice used in these studies. The specific CRISPR-targeted exons (those with homology to the ITIM) were Sanger sequenced as representative of the most likely position of off-target effects and to confirm and characterize the frameshift in on-target variants. The primers used for PCR and subsequent sequence analysis are shown in **Table S4**. (A-P) Each panel depicts the reference sequence (above), the region of the exon targeted (in blue), the on-target and off-target guide sites (in purple), and the Sanger alignments (below) for the mice indicated. Mice are designated as to which strains (in parentheses) were analyzed. B6 is the wild-type genome for comparison. Red boxes indicate indels (inserted nucleotides are shown, while deleted bases are represented as a dash). Sequence analysis was confirmed in both the forward and reverse directions, however, for clarity only one direction is shown. Sequences assessed in each panel are as follows: (A) *Klra1/Ly49a*, (B) *Klra2/Ly49b*, (C) *Klra3/Ly49c*, (D) *Klra4/Ly49d*, (E) *Klra5/Ly49e*, (F) *Klra6/Ly49f*, (G) *Klra7/Ly49g*, (H) *Klra8/Ly49h*, (I) *Klra9/Ly49i*, (J) *Klra10/Ly49j*, (K) *Klra11-ps/Ly49k*, (L) *Klra13-ps/Ly49m*, (M) *Klra14/Ly49n*, (N) *Klra17/Ly49q*, (O) *Gm6548*, and (P) *Gm15854/Ly49x*. (Q) Nucleotide level analysis of the ΔLy49-1 deletions for the haplotype corresponding to **Figure 2A** at the *Ly49g-Ly49a* and *Ly49n-Ly49k* junctions. Related to **Figure 2A**.

Figure S2. Flow cytometric characterization of CRISPR-Cas9 modified mice.
Offset flow histograms are shown for mice on the D8-KODO (H2D^{d}) MHC background with the indicated CRISPR-Cas9 modifications. Single-cell suspensions of mouse splenocytes were gated for expression of specific proteins with loci near or in the NKC. (A-O) Shown is a representative plot of NK1.1^{+}/NKp46^{+}/CD19^{-}/CD3^{-} lymphocytes. Protein levels assessed in each panel are as follows: (A) Ly49A, (B) Ly49C, (C) Ly49D, (D) Ly49EF, (E) Ly49F, (F) Ly49G, (G) Ly49H, (H) Ly49I, (I) CDD94, (J) NKG2A, (K)

NKG2D, (L) CD69, (M) CD122, (N) CD127 and (O) 2B4. The flow cytometric analyses were repeated twice with 3 mice per group. Below the plots, quantification of the flow data as frequencies (A-J) or MFI (K-O) from one of two representative experiments is provided. (P) Representative maturation plots are shown for all experimental mice with the summation of a representative experiment provided at the bottom. No significant deviations were noted. Analyses were repeated twice with 3 mice per group. (Q) Quantification of NK cell frequencies gated as $CD3^{-}CD19^{-}NK1.1^{+}$ lymphocytes. (R) Flow cytometric analysis of mice heterozygous for the ΔLy49-1 D8-KODO KO (F_1 hybrids of KODO mice with intact *Ly49*s and ΔLy49-1 D8-KODO mice from **Fig2B**) compared with KO and WT mice. Experiments were performed twice with 5-7 mice per group, with the exception that WT mice were assessed only once in this panel with values consistent with panels above. (S) Flow cytometry gating strategy. For all flow cytometry data, statistical analyses was performed using one-way ANOVA and corrected for multiple comparison using the Bonferroni method with D8-KODO expression or MFI as a comparator; ****$p < .0001$, ***$p < .001$, **$p < .01$, *$p < .05$. Related to **Figures 2** and **4**.

Figure S3. Strategy and characterization of the NKp46-Ly49A knockin.

(A) CRISPR knockin strategy for Ly49A expression on NKp46-expressing cells. 2 CRISPR guides, T1 and T3 (**Table S1**) were injected into B6 zygotes along with Cas9 mRNA and a donor DNA construct engineered to express the *Ly49A* cDNA following a P2A cleavage site such that the Ly49A expression would be proportional to NKp46 (*Ncr1*) transcript levels. (B) The final NKp46 TGA stop codon and several downstream bases (yellow highlighted region) in the coding region of exon 7 (blue text) were removed and replaced with a P2A site (purple text), Ly49A cDNA (red text) and finally the remainder of the NKp46 3' UTR sequence (green text). This donor vector with NKp46 homologous arms was co-injected with sgRNA for *Ncr1* and Cas9 into B6 zygotes and positive knockin mice were selected at birth by PCR analysis and confirmed at 6 weeks of age by flow cytometry. (C) One Ly49A KI line was crossed to the

ΔLy49-1 D8-KODO mice (**Figure 2A**) heterozygous for one knockin allele and confirmed by flow cytometry. Lymphocytes for splenic single cell suspensions were assessed for both NK1.1 and Ly49A expression. Approximately 18% of NK cells from WT (D8-KODO) mice expressed Ly49A, while the ΔLy49-1 D8-KODO mice lacked all Ly49A expression unless expressing the Ly49A from the knockin construct (nearly 100% expression). As shown, Ly49A expression was restricted to $NK1.1^{+}$ splenocytes. Related to **Figures 3F** and **4C**.

Figure S4. *In vivo* cytotoxicity in Ly49AG KO and Ly49AYF mice.

In vivo cytotoxicity of MHC-I deficient (KODO) or sufficient (D8-KODO) splenocytes following differential labelling with Celltrace Violet and flow cytometric analysis recovered from spleens at 2 days post-injection. (A) Flow cytometric analysis of input cells is shown (prior to injection). The experimental design is also depicted with the timing of antibody depletion relative to injection and harvest. (B) Representative histogram plots of the mice indicated in each row and treatments by column. The peaks are identified by the input plot shown in (A). (C) Quantification was performed as previously described (**Figure 4C**). Data are representative of two independent experiments with three recipient mice per group that received the same mix of donor cells in each experiment. Standard error of the mean is shown; statistical analysis performed using one-way ANOVA and corrected for multiple comparison using the Bonferroni method; $*p < .05$, $****p < .0001$. Related to **Figure 4**.

Figure S5. Sanger sequence analysis of *m06* and *m152* in CRISPR-modified MCMV strains.

Viral DNA was isolated from *in vitro* cell cultures infected with CRISPR-Cas9 modified MCMV used in these studies. The specific CRISPR-targeted ORFs, (A) *m06* and (B) *m152*, were Sanger sequenced to confirm and characterize the frameshift in on-target variants. The primers used for PCR and subsequent sequence analysis are shown in **Table S5**. Each panel depicts the reference sequence above with the

region of the ORF expanded for analysis. The Sanger alignments below for the viruses indicated are designated as to which strains (*left* of trace) were analyzed. Δm157-MCMV is the wild-type genome at these ORFs, for comparison. Red boxes indicate where inserted nucleotides were identified. Sequence analysis was confirmed in both the forward and reverse direction, however, only one direction is shown for clarity. Related to **Figure 5**.

Figure S6. Multi-step growth curve

Multi-step *in vitro* growth kinetics of two strains of MCMV, as indicated. Cells and supernatants were harvested at the indicated days and quantified by real-time PCR. Data is a representative of two independent experiments with each data point performed in triplicate. All timepoints were shown to significantly different in terms of viral load ($p < .0001$); statistical analysis performed with a Student's *t*-Test. Related to **Figure 5**.

A.

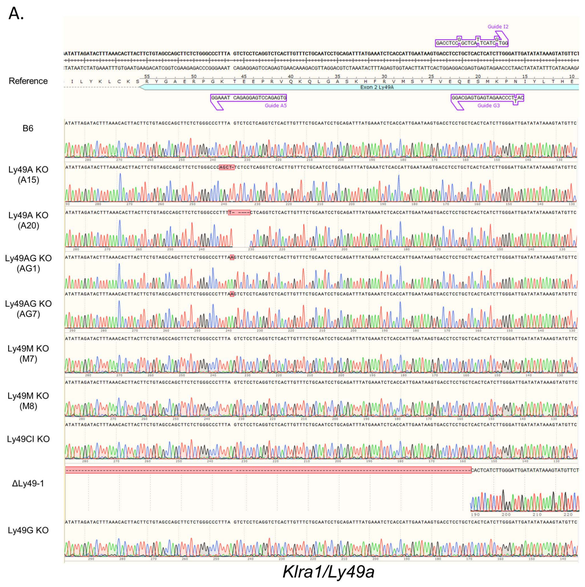

Klra1/Ly49a

B.

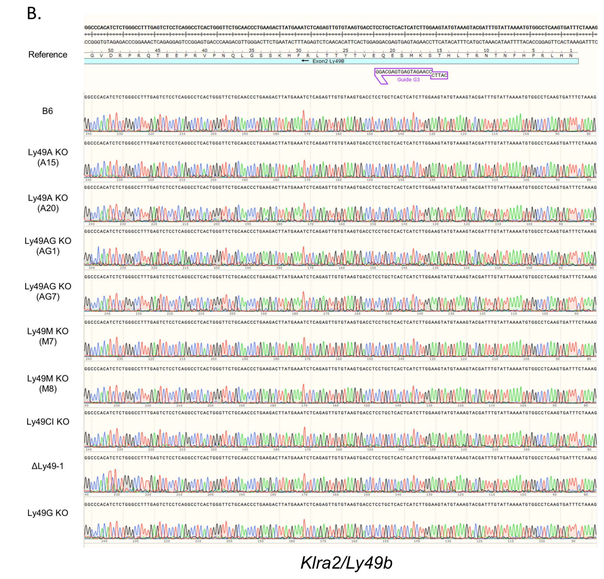

Klra2/Ly49b

C.

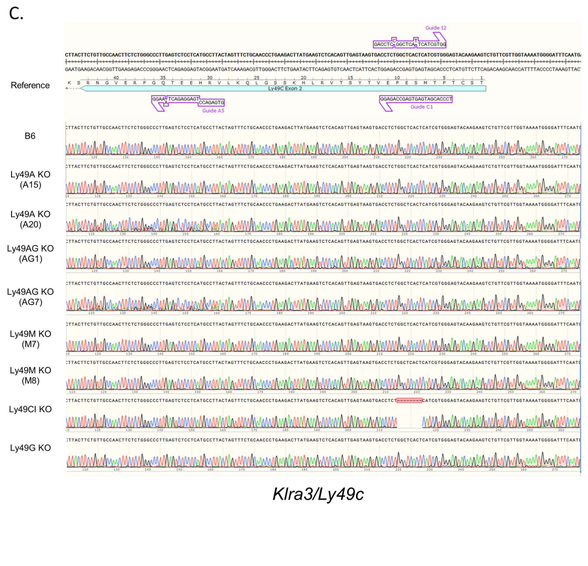

Klra3/Ly49c

D.

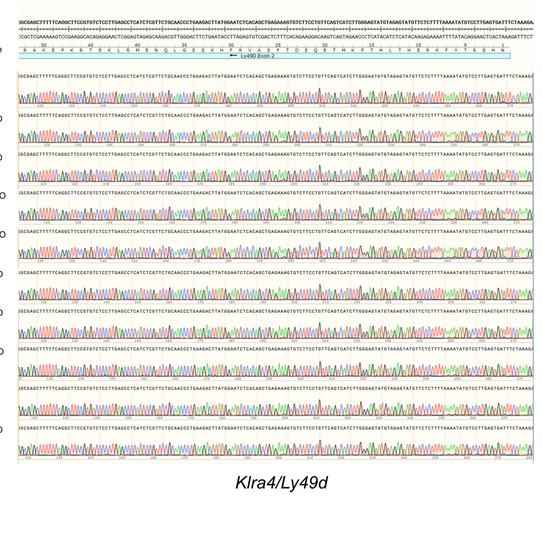

Klra4/Ly49d

E.

Klra5/Ly49e

F.

Klra6/Ly49f

G.

Klra7/Ly49g

H.

Klra8/Ly49h

I.

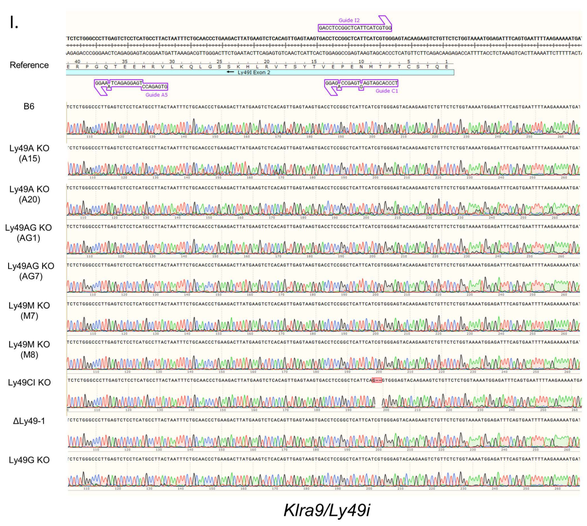

Klra9/Ly49i

J.

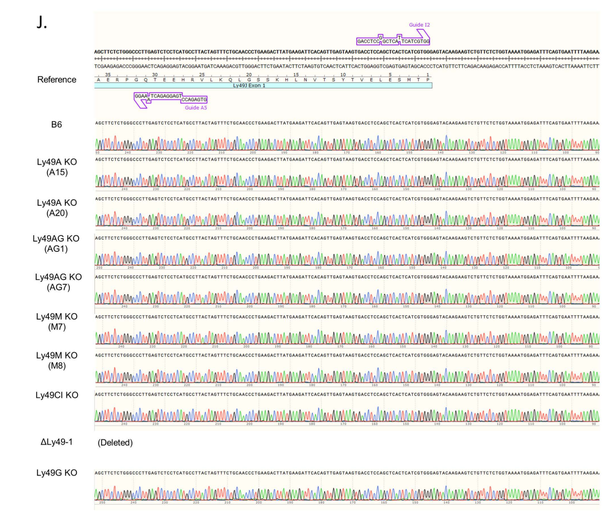

Klra10/Ly49j

K.

Klra11-ps/Ly49k

L.

Klra13-ps/Ly49m

M.

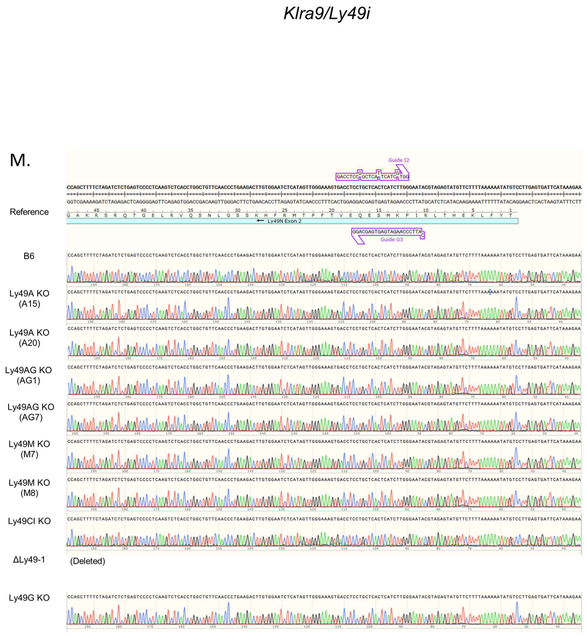

Klra14-ps/Ly49n

N.

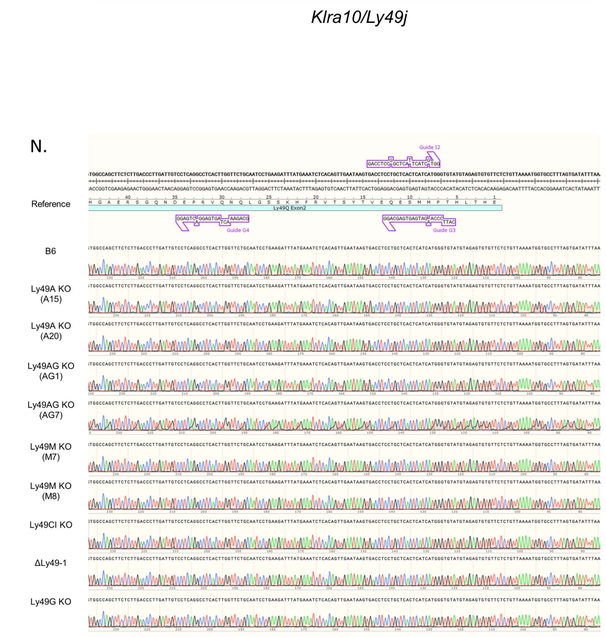

Klra17/Ly49q

O.

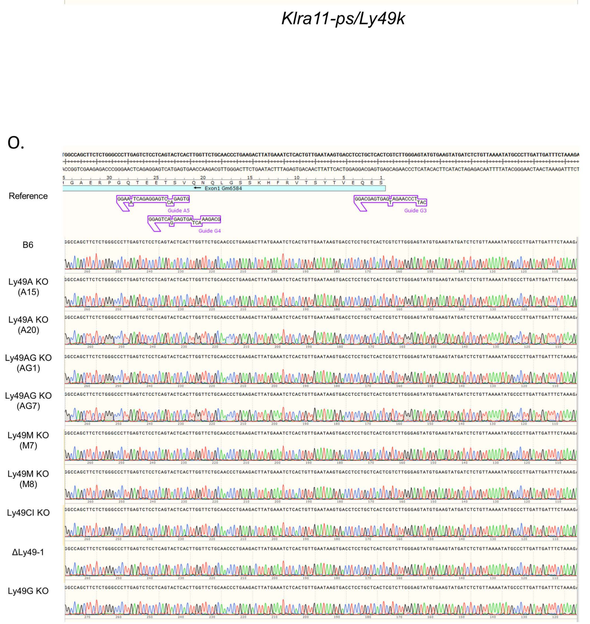

Gm6584

P.

Gm15854/Ly49x

Q.

ΔLy49-1

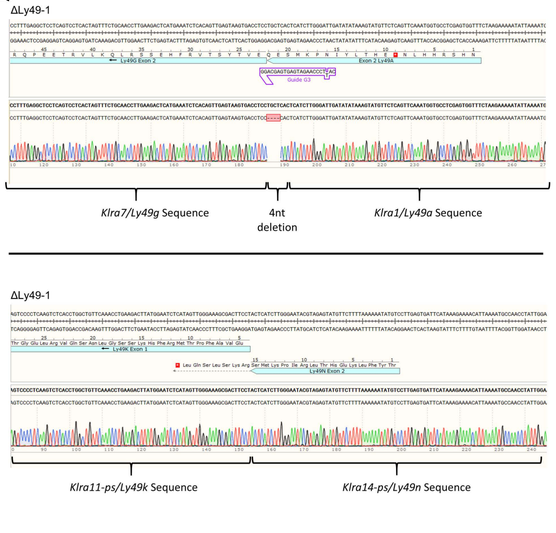

Klra7/Ly49g Sequence | 4nt deletion | *Klra1/Ly49a* Sequence

ΔLy49-1

Klra11-ps/Ly49k Sequence | *Klra14-ps/Ly49n* Sequence

A.

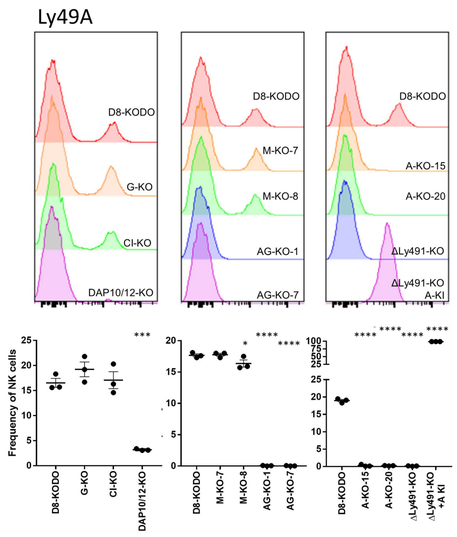

B.

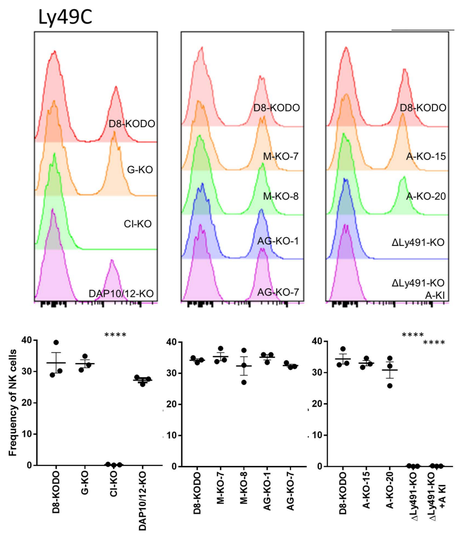

C.

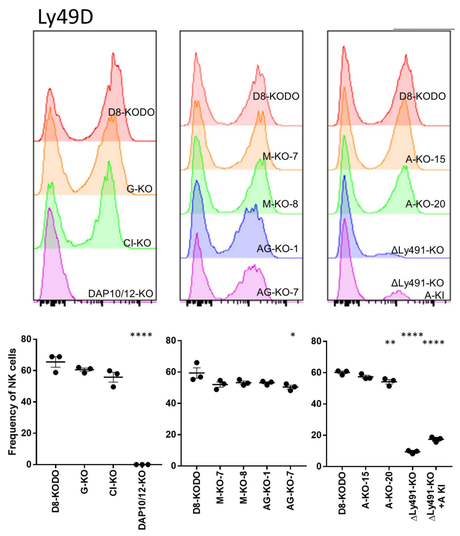

D.

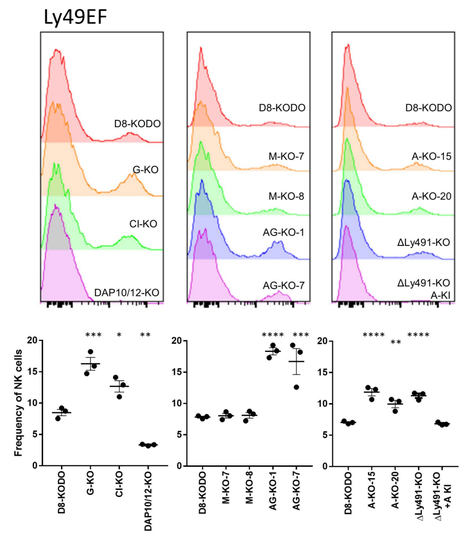

E.

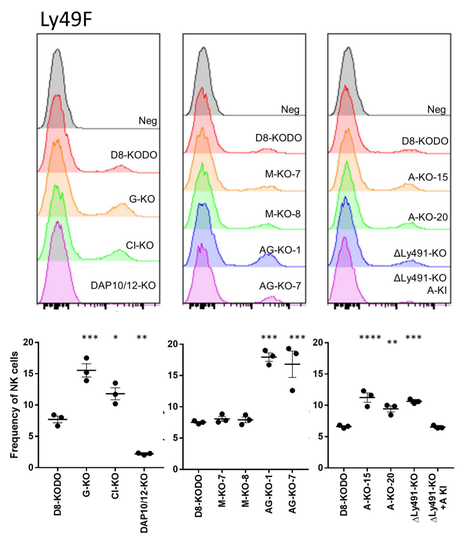

F.

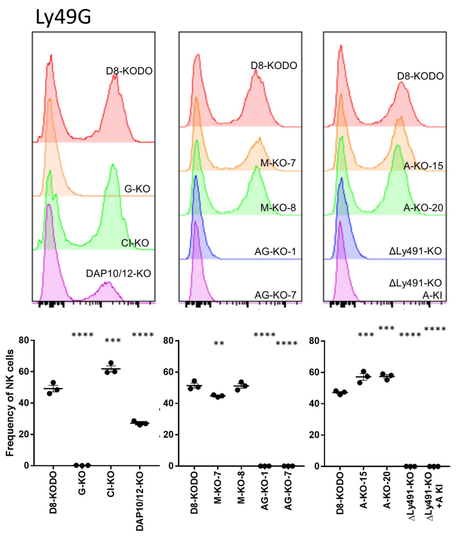

G.

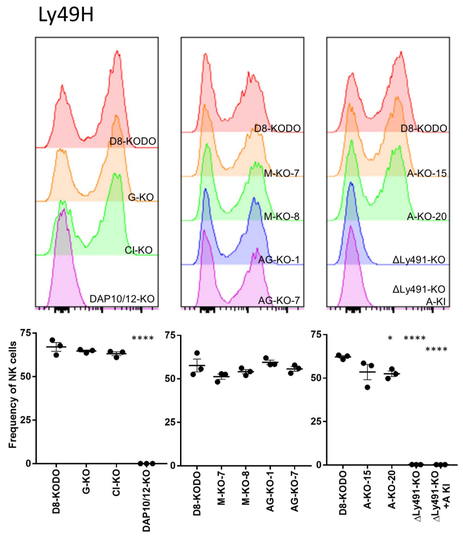

H.

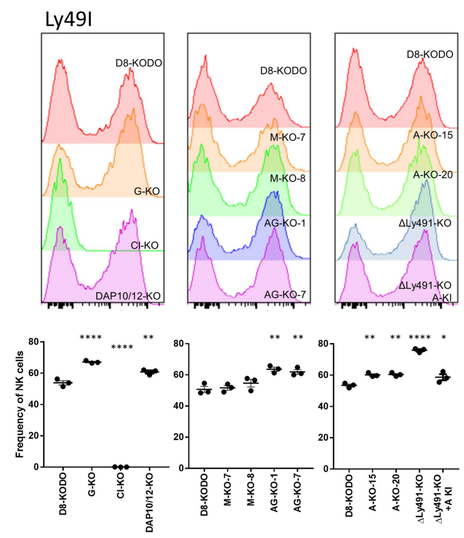

I.

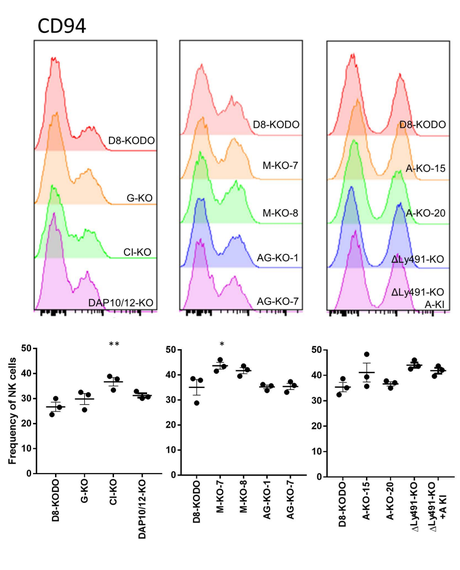

J.

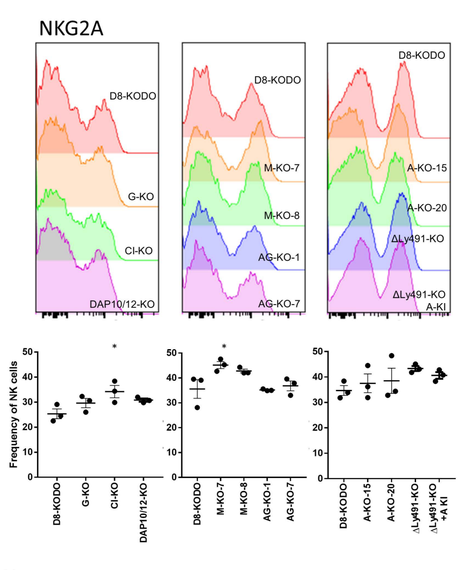

K.

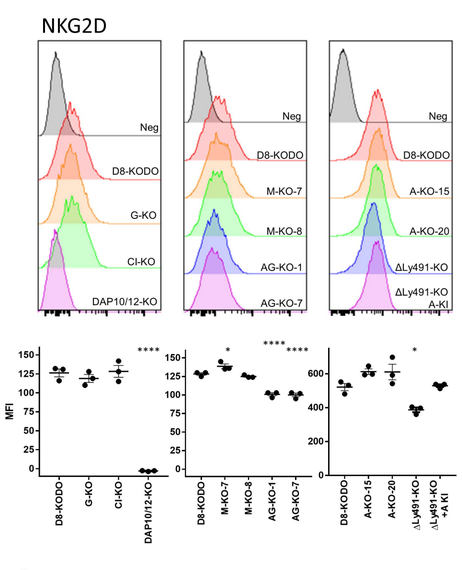

L.

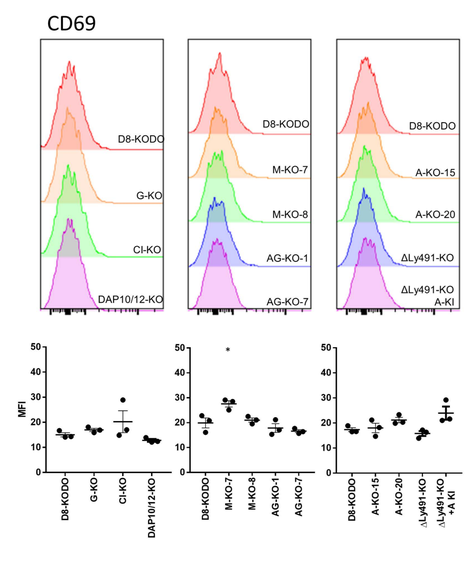

M.

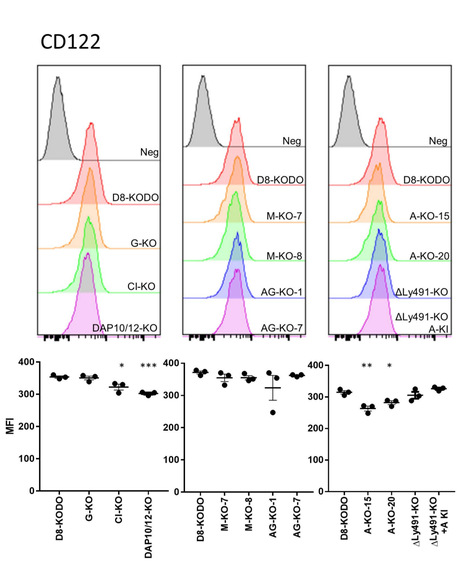

N.

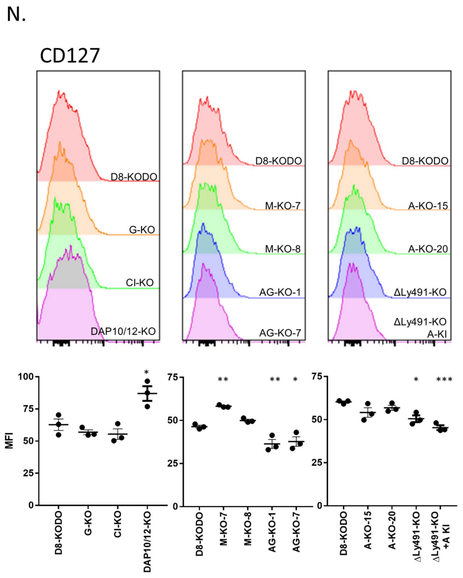

O.

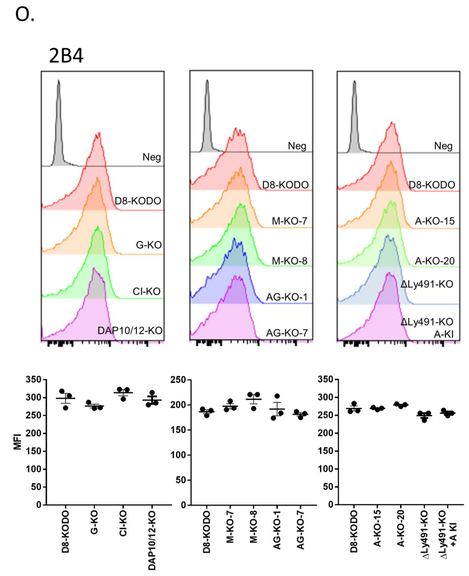

P.

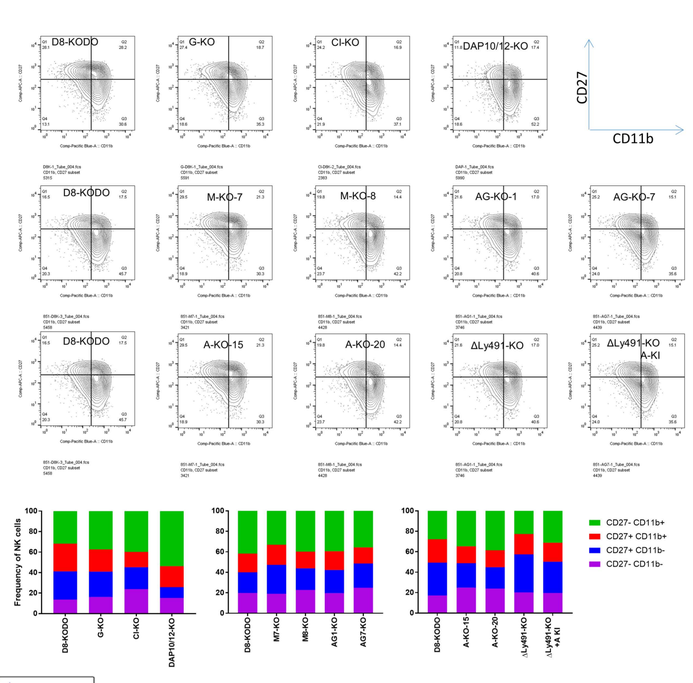

Q.

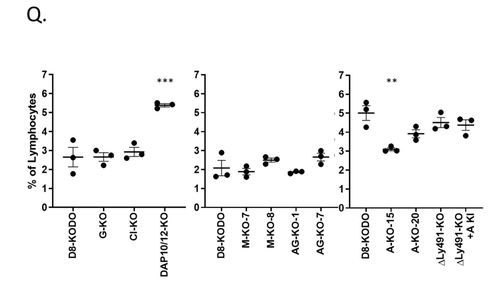

R.

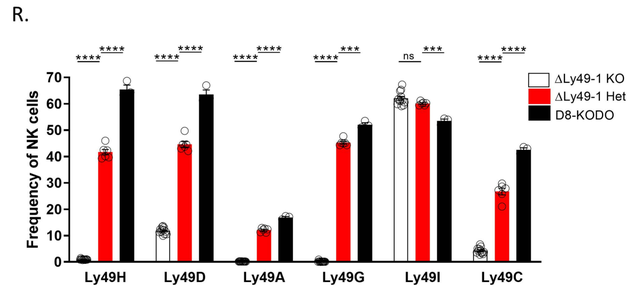

S.

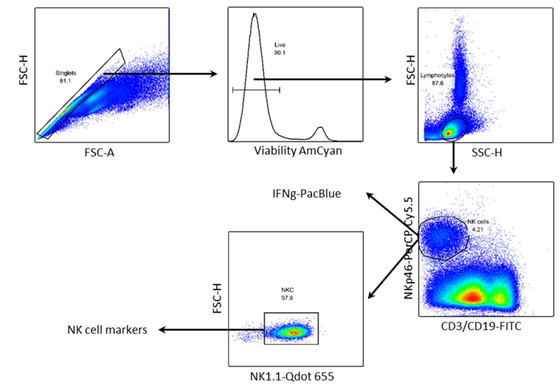

A.

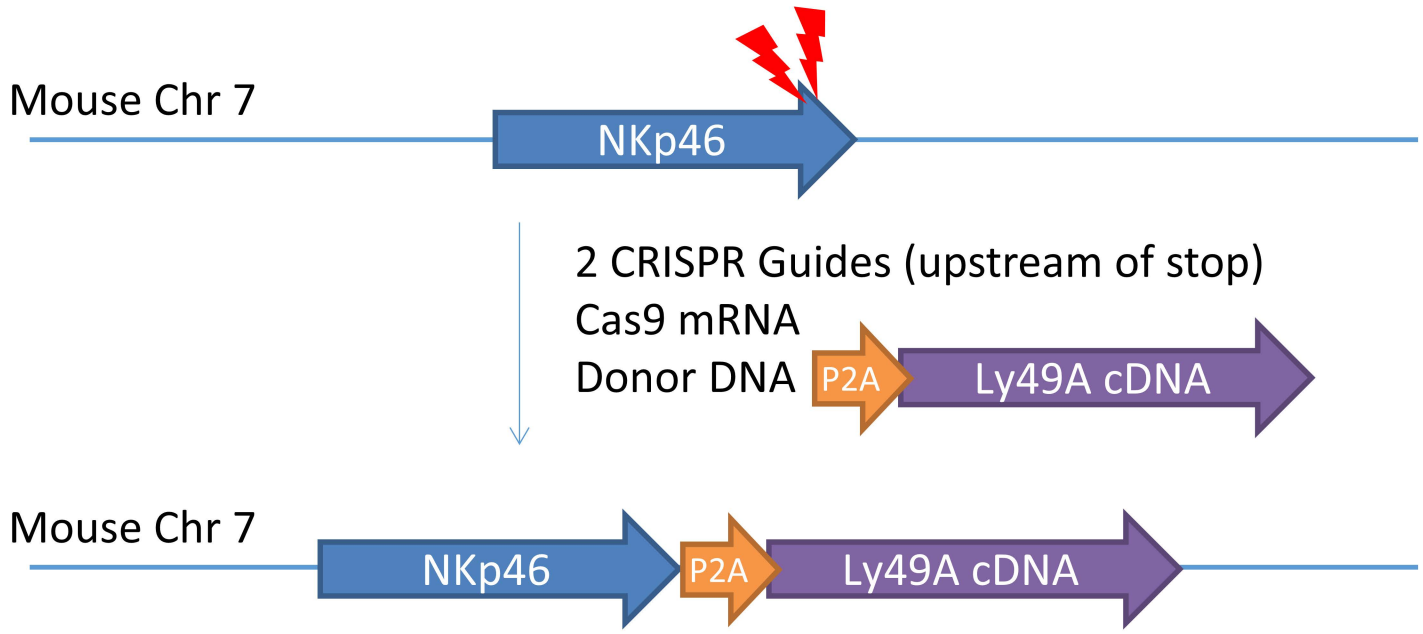

B.

Segment of chr7:4344460-4345184 (GRCm38/mm10)
Exon 7 coding region of Ncr1 / 3' UTR of Ncr1
Replaced with P2A-Ly49A cDNA

actccgccttctgggatcacacaacccagaatctcattcgaattggtctggcatgcataatcctgataactctagtatggcttttgactgaagactg
gctcagcaagaggaaagatcatgaagaggccaacagattaacaaattggaatgcaggagaagatggagaatgcagcattactttgaaga
ggaacaaagaaatgcaatatctatgatggaactgaaggcaactcctggggcattgtgagctctatgctgtaccctggataaagaaagagatct
tttcagaaatgaaggggtaggagtgttaccaagtttggcaaagcattctaaaggacactgtgagaggaagcctctaacagacctctctgtctct
gctaagctttaagtactttaacgcttatttactgcaagttatacttttgatcactctggtctttcctagaaataacttcgttccaatgtgatggccatggga
atatttccttcctactttaggtcttatcgtcatttctttttctaattttatttatttttatgttgccgggaattgaactcaagttgtctggaggagcaacaagtgct
cttaactacaaaccatatctccagctccatcctcaatattttatattgtgtgtgcatgtctgtaggatgcatgtgtgtgcacacatatgtacatatattct
atgccattaaaatgaaggtcagagaacacctctgtgaagtca

ggatctggagcaacaaacttctcactactcaaacaagcaggtgacgtggaggagaatcccgggcctatgagtgagcaggaggtcacttattc
aatggtgagatttcataaatctgcaggattgcagaaacaagtgagacctgaggagactaaagggcccagagaagctggctacagaaggtg
ttcattccactggaagttcattgtgatagctcttggcatcttctgtttccttcttctggtagctgtttcagtgttggcaataaaaatttttcagtatgatcaac
aaaaaaaactgcaggaatttctaaaccaccacaataactgcagcaacatgcaaagtgacatcaacttgaaggatgaaatgctgaaaaata
agtctatagagtgtgatcttctggaatccctcaacagggatcagaacagattgtataataaaaccaagactgttttagattccttacagcacaca
ggcagaggtgataaagtatactggttctgctatggtatgaaatgttattatttcgtcatggacagaaaaacatggagtggatgtaaacagacctg
ccagagttccagtttatcccttctgaagatagatgatgaggatgaactgaagttccttcagctcgtggttccttcagacagttgctgggttggattgtc
atatgataataagaaaaaagattgggcatggattgacaatcgcccatctaaacttgccttgaacacaaggaaatacaatataagagatgggg
gatgtatgttgttatctaaaacaagactagacaatggtaactgtgatcaagtattcatctgtatttgtgggaagagactggataaattccctcattga

C.

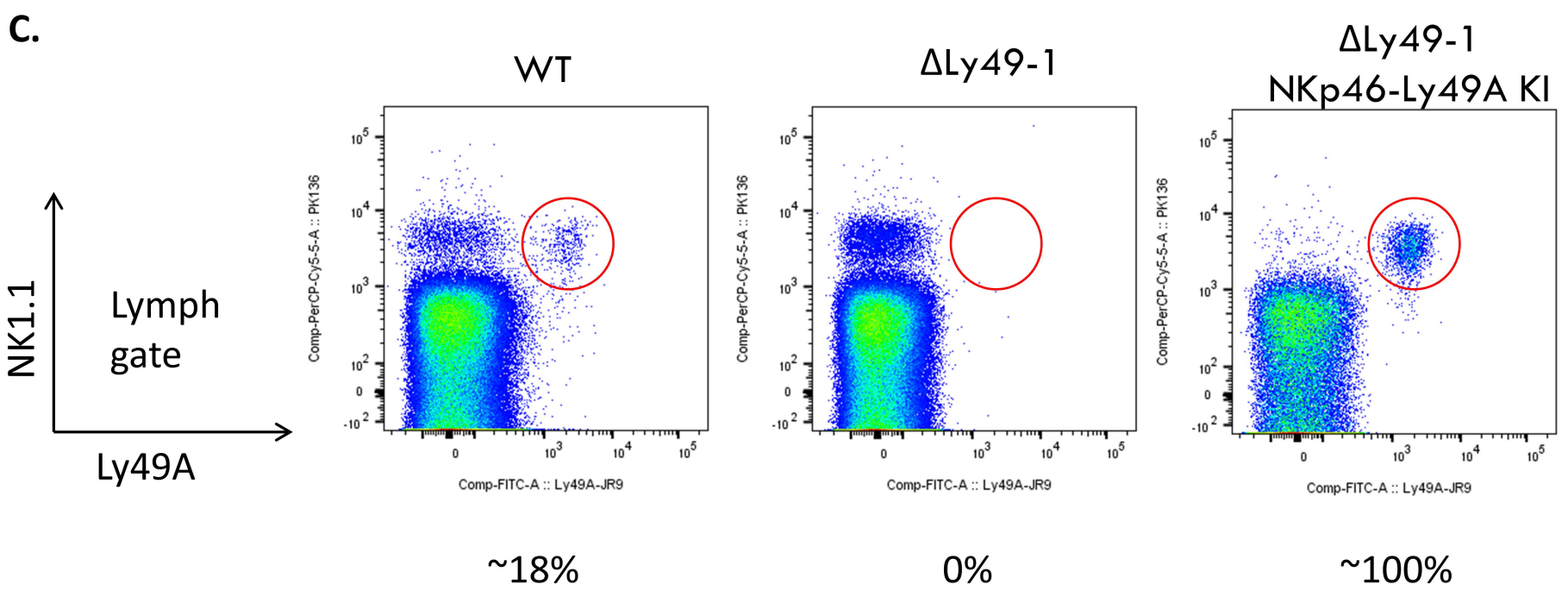

A.

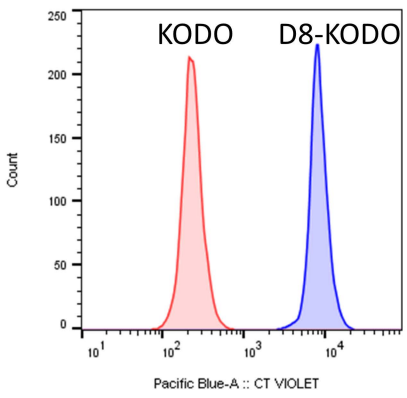
Input
KODO
D8-KODO
Count
Pacific Blue-A :: CT VIOLET

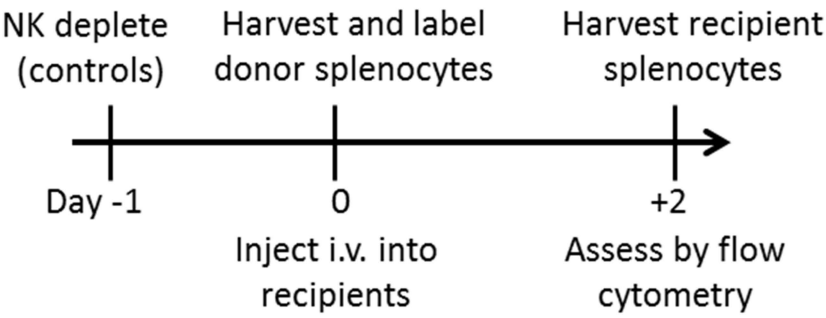
NK deplete (controls)
Harvest and label donor splenocytes
Harvest recipient splenocytes
Day -1
0
+2
Inject i.v. into recipients
Assess by flow cytometry

B.

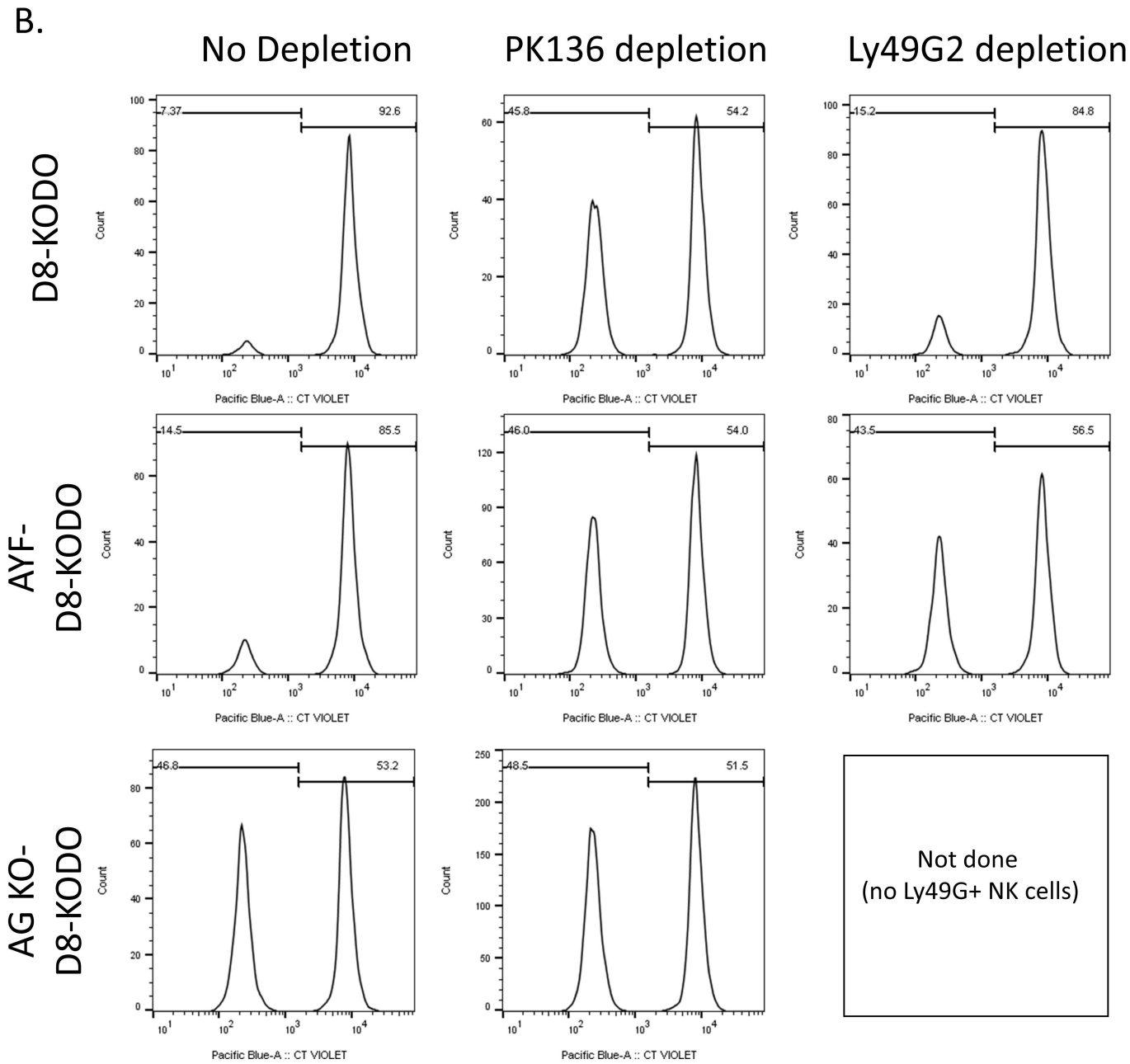
No Depletion
PK136 depletion
Ly49G2 depletion
D8-KODO
AYF-D8-KODO
AG KO-D8-KODO
7.37
92.6
45.8
54.2
15.2
84.8
14.5
85.5
46.0
54.0
43.5
56.5
46.8
53.2
48.5
51.5
Count
Pacific Blue-A :: CT VIOLET
Not done
(no Ly49G+ NK cells)

C.

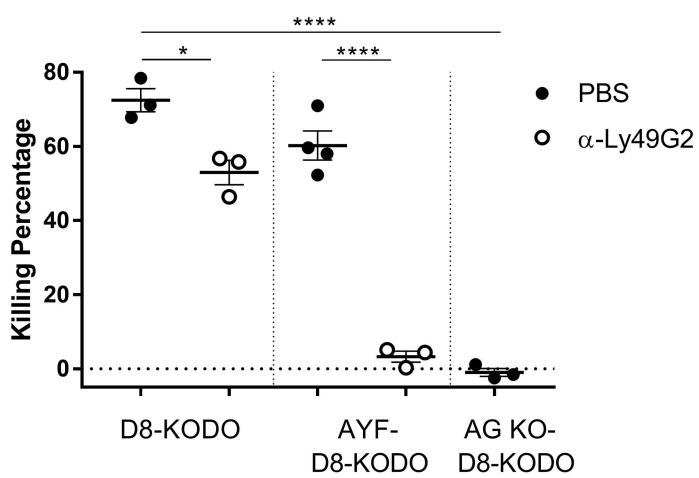
****
*
****
Killing Percentage
PBS
α-Ly49G2
D8-KODO
AYF-D8-KODO
AG KO-D8-KODO

A.

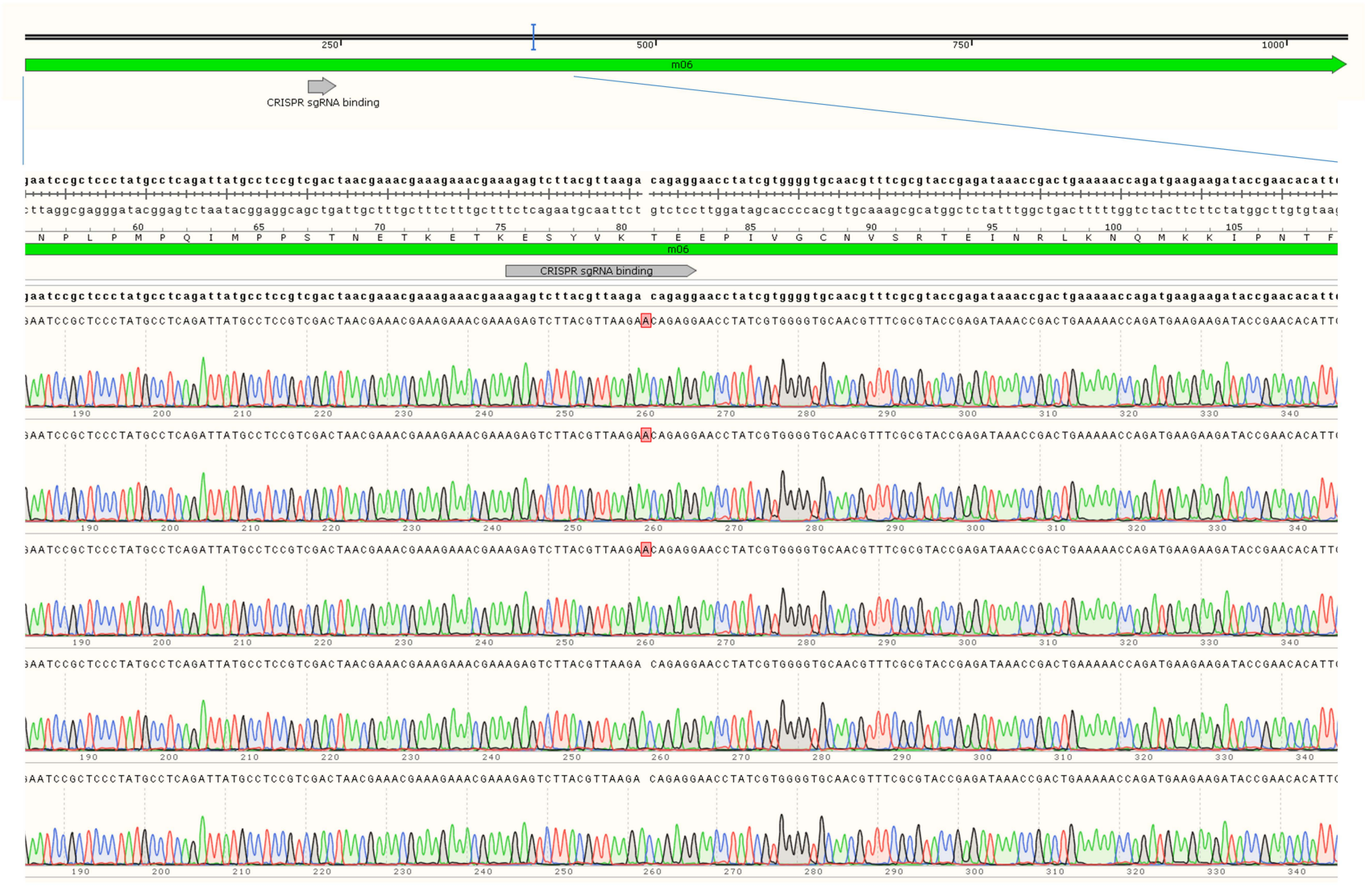
m06
CRISPR sgRNA binding
GFP-MCMV Δm06
GFP-MCMV Δm06/ Δm152
Δm157-MCMV Δm06/Δm152
GFP-MCMV Δm152
Δm157-MCMV

B.

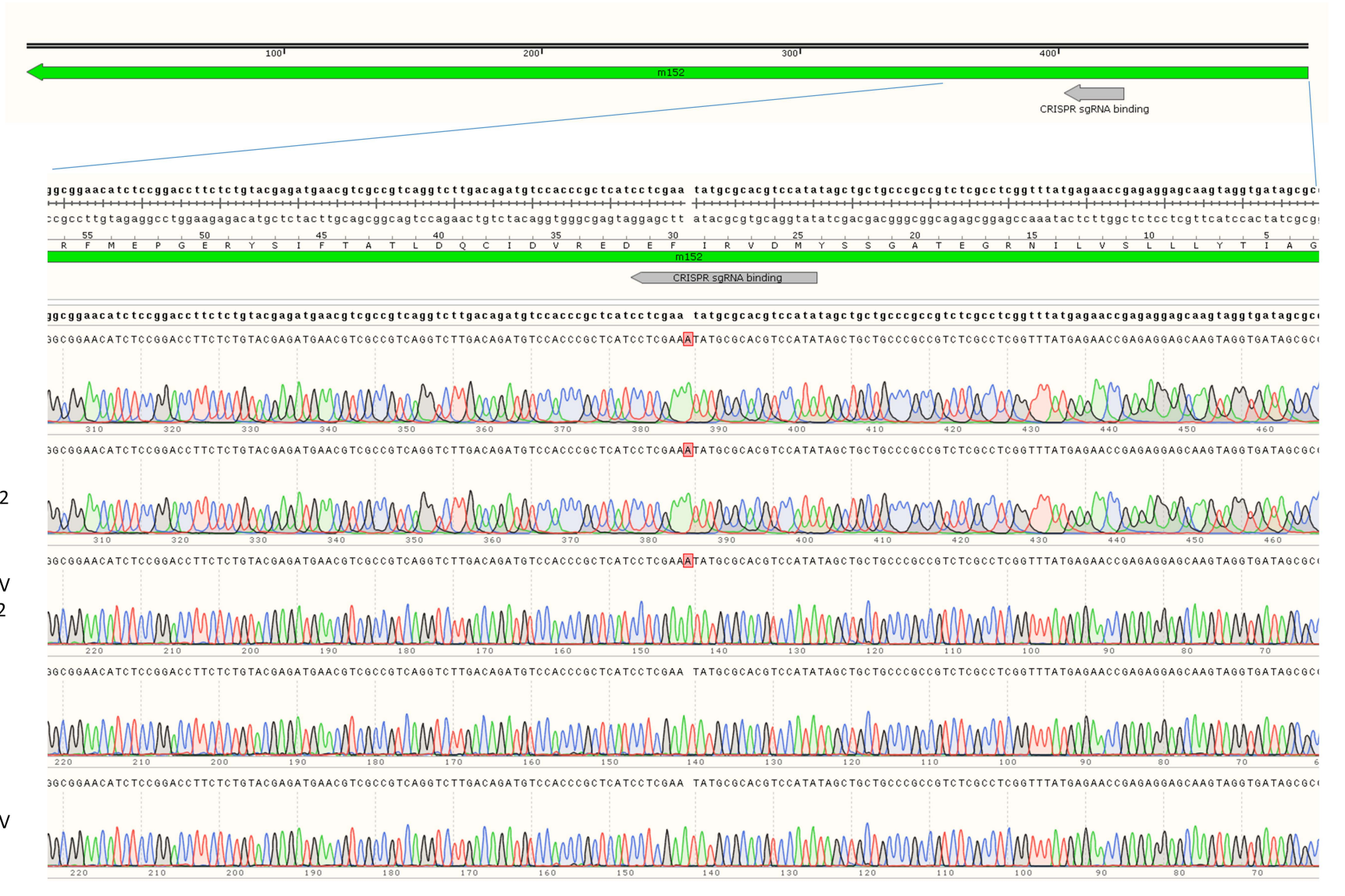
m152
CRISPR sgRNA binding
GFP-MCMV Δm152
GFP-MCMV Δm06/ Δm152
Δm157-MCMV Δm06/Δm152
GFP-MCMV Δm06
Δm157-MCMV

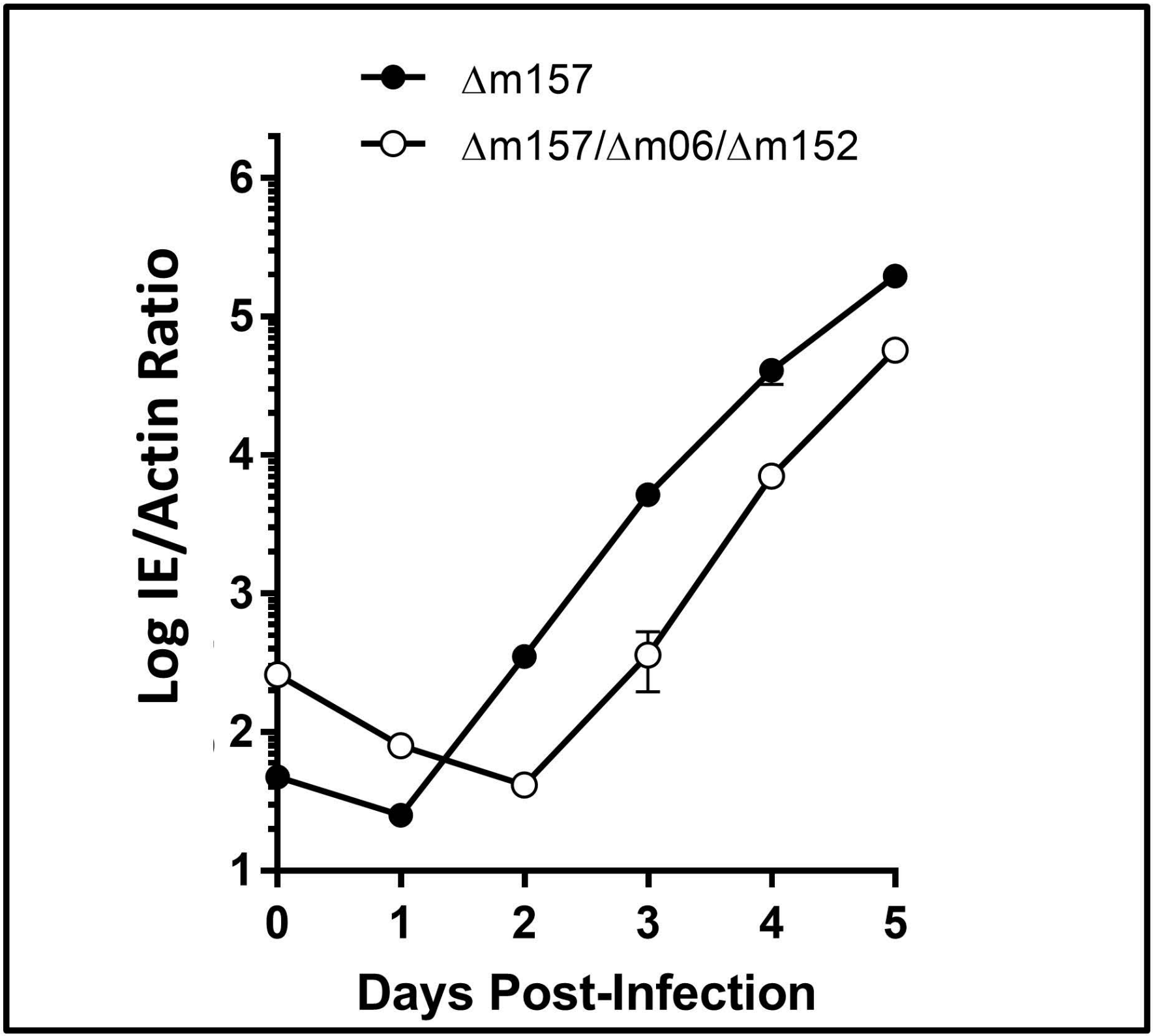
Δm157
Δm157/Δm06/Δm152
Log IE/Actin Ratio
6
5
4
3
2
1
0
1
2
3
4
5
Days Post-Infection

Supplementary Tables

Table S1: sgRNA used in generation of CRISPR-Cas9 modified mice

Guide ID	Target	Sequence + PAM	Mouse Generated	Chr
G3	*Ly49g/a/h*	CATTCCCAAGATGAGTGAGCAGG	ΔLy49-1	6
I2	*Ly49i*	GACCTCCGGCTCATTCATCGTGG	C14B	6
C1	*Ly49c*	TCCCACGATGAGTGAGCCAGAGG	C14B	6
M1	*Ly49m*	CGGGTGAGGCTTGAGGAGACAGG	M1, M4, M7, M8	6
G4	*Ly49g*	GCAGAAACTAGTGAGGACTGAGG	AG1, AG7	6
A5	*Ly49a*	GTGAGACCTGAGGAGACTAAAGG	AG1, AG7, A15, A20	6
T3	*Ncr1*	GGTACAGCATAGAGCTCACAAGG	Ly49A-KI	7
T1	*Ncr1*	GTGAGCTCTATGCTGTACCCTGG	Ly49A-KI	7

The names of the sgRNA guides (Guide ID) are provided along with the intended genomic targets, the sgRNA sequence including the "NGG" protospacer adjacent motif (PAM) site underlined, the mice generated with the sgRNA and the chromosomal location of the targeted gene. A complete list containing all relevant on-target and off-target sites in B6 mice is provided as supplemental file **Table_S1.xls** and references the specific guides using the Guide ID. In this file, individual on-target and potential off-target sites are indicated as identified by CCTop (see Methods). Specifically, the input sgRNA sequence along with the number of mismatches and the location of mismatches within the 12nt core (less likely to bind) or outside the core are shown. Chromosome positions of targets along with gene names, if available are indicated. Potential off-target sites within the target chromosome are highlighted and were carefully examined with sequence (**Figure S1**) and flow cytometric methods (**Figure S2**). Related to STAR Methods.

Table S2: List of MCMV sgRNA target sites

A complete list of all guides with no or minimal off-target sites is provided as supplemental file **Table_S2.xls.** In this file, individual on-target and potential off-target sites are indicated as identified by CCTop (see Methods). Specifically, the individual sgRNA sites only within the MCMV genome was interrogated for all CRISPR/Cas9 target sites. Any alternate cleavage sites are indicated. The two sgRNA guide sequences used in our experiments are identified as T303 (*m06*) and T18561 (*m152*) (see also **Table S3**) and is highlighted in yellow within the file. Related to STAR Methods.

Table S3: sgRNAs specific for MCMV *m06* or *m152*

Guide ID	Target	sgRNA Sequence + PAM	Forward Oligo (5' to 3')	Reverse Oligo (5' to 3')
T303	*m06*	AGAGTCTTACGTTAAGACAGAGG	caccgAGAGTCTTACGTTAAGACAG	aaacCTGTGTTAACGTAAGACTCTc
T18561	*m152*	TATGGACGTGCGCATATTCGAGG	caccgTATGGACGTGCGCATATTCG	aaacCGAATATGCGCACGTCCATAc

The names of the sgRNA guides (Guide ID) are provided (see also **Table_S2.xls**) along with the intended MCMV ORF targets, and the sgRNA sequence including the "NGG" protospacer adjacent motif (PAM) site underlined. Two oligos were used to generate duplex DNA used for cloning into the modified px330 *Cas9*-encoding vector (see **Methods**). An additional guanine residue was appended to the forward oligo (and complementary cytosine to the reverse oligo) to enhance sgRNA production from the *U6* promoter in cells. Related to STAR Methods.

Table S4: The primers used for *Ly49* gene sequence analysis

Gene	Fwd Primer Sequence (5' to 3')	Rev Primer Sequence (5' to 3')	Amplicon size (nt)
Klra1/Ly49a	TCTTCCCTCCCATCTTTGTTCA	TGGGTCAGTCCATGTCAGTG	439
Klra2/Ly49b	ATTGTTCTGCTCTGCGCATC	AGAGTCAGGGTGTTTGGACC	409
Klra3/Ly49c	TCTTCCCTCCCGTCCTTGTA	TGCATGTCAGGGTGTTTGGA	428
Klra4/Ly49d	TCACCCTCATGCATAACTAAGG	CAGTCCATGCTGCAGTGTTT	421
Klra5/Ly49e	CTTCTCCGGGCCCTTGAATC	GGCTGTATCAATGGTAGAATGGC	414
Klra6/Ly49f	CTCCCATACTTGTGCATAATCAAA	GGATCAGTCCATGTCAGGGTG	427
Klra7/Ly49g	AACCAAGCCCCAATGAGATC	GGTCAGTCCATGTCAGGGTG	411
Klra8/Ly49h	GGAACATTTTACTTTTCAATGAAAGCCT	CTGTATCATCAGATCCAGGTACCTTT	324
Klra9/Ly49i	CAAGCCCCGATGAGATGGAT	GGATCAGTCCATGTCAGGGTT	409
Klra10/Ly49j	CAAGCCCCGATGAGATGGAC	GGATCAGTCCATGTCAGGGTA	409
Klra13-ps/Ly49m	CTTTTCTTCTCTCTCACCCTTATGCATAAC	CCCAAGATGAGTGAGCAGGAGGT	278
Klra14-ps/Ly49n	ACTTCTTGTTTCCCAAGAAATGTTTTCTTACTG	CACCCTTTCTCAACCTTCTGTATCACT	591
Klra17/Ly49q	GCCCATCTGGCTTCCTTTCT	TGAGTCCCAGTCAGGGTCAT	533
Gm15854/Ly49x	TTCTCTCTTACCCTCGTGCATAAC	GTGAGGTCAGTCCATGCTGAG	438
Gm6584	AGCCAAGCCCAGATGAAATGA	ACAGGGTTTCTCCCCTGAAA	428

This table provides the primer sequences and amplicon lengths used for amplification and sequencing the *Ly49* region of the murine NKC locus on chromosome 6. See **Methods** for sequencing conditions and **Figure S1** for results. Related to STAR Methods.

Table S5: The primers used for MCMV *m06* and *m152* gene sequence analysis

ORF	Fwd Sequence Primer (5' to 3')	Rev Sequence Primer (5' to 3')	Amplicon size (nt)
m06	CACGCCCAAAATCACGCAAAC	GGCGTAGTCGAATGGTACA	853
m152	CGATGTCATCCTCGGATA	GGCTACTCCCGAAAGAGTAA	578

This table provides the primer sequences and amplicon lengths used for amplification and sequencing the viral ORFs *m06* and *m152* from MCMV. See **Methods** for sequencing conditions and **Figure S5** for results. Related to STAR Methods.